Postnatal TrkB ablation in corticolimbic interneurons induces social dominance in male mice

Shawn Tan[a,b,c], Yixin Xiao[a], Henry H. Yin[d], Albert I. Chen[e,f,g], Tuck Wah Soong[b,c], and H. Shawn Je[a,c,1]

[a]Program in Neuroscience and Behavioral Disorders, Duke–National University of Singapore Medical School, Republic of Singapore 169857; [b]Graduate School for Integrative Sciences and Engineering, National University of Singapore, Republic of Singapore 117456; [c]Department of Physiology, Yong Loo Lin School of Medicine, National University of Singapore, Republic of Singapore 117597; [d]Department of Neurobiology, Duke University Medical Center, Durham, NC 27710; [e]School of Biological Sciences, Nanyang Technological University, Republic of Singapore 636921; [f]School of Life Sciences, University of Warwick, Coventry CV4 7AL, United Kingdom; and [g]Institute of Molecular and Cell Biology, Agency for Science, Technology and Research (A*STAR), Republic of Singapore 138673

Edited by Hee-Sup Shin, Institute for Basic Science, Daejeon, Republic of Korea, and approved September 11, 2018 (received for review July 16, 2018)

The tight balance between synaptic excitation and inhibition (E/I) within neocortical circuits in the mammalian brain is important for complex behavior. Many loss-of-function studies have demonstrated that brain-derived neurotrophic factor (BDNF) and its cognate receptor tropomyosin receptor kinase B (TrkB) are essential for the development of inhibitory GABAergic neurons. However, behavioral consequences of impaired BDNF/TrkB signaling in GABAergic neurons remain unclear, largely due to confounding motor function deficits observed in previous animal models. In this study, we generated conditional knockout mice (TrkB cKO) in which TrkB was ablated from a majority of corticolimbic GABAergic interneurons postnatally. These mice showed intact motor coordination and movement, but exhibited enhanced dominance over other mice in a group-housed setting. In addition, immature fast-spiking GABAergic neurons of TrkB cKO mice resulted in an E/I imbalance in layer 5 microcircuits within the medial prefrontal cortex (mPFC), a key region regulating social dominance. Restoring the E/I imbalance via optogenetic modulation in the mPFC of TrkB cKO mice normalized their social dominance behavior. Taken together, our results provide strong evidence for a role of BDNF/TrkB signaling in inhibitory synaptic modulation and social dominance behavior in mice.

social dominance | prefrontal cortex | BDNF | TrkB | interneurons

Brain-derived neurotrophic factor (BDNF) and its cognate receptor, tropomyosin receptor kinase B (TrkB), play a fundamental role in brain development, including neuronal maturation, dendritic remodeling, formation of synaptic contacts, and synaptic plasticity (1–3). More importantly, studies have identified that BDNF is indispensable for the long-term survival and maintenance of cortical GABAergic interneurons (4–6). For example, in cortical cell cultures, BDNF promotes neurite growth of GABAergic neurons, up-regulates GABA synthesis and several calcium-binding proteins that are unique to GABAergic neurons, and regulates the strength of synaptic inhibition (7–10). Furthermore, both genetic reduction of BDNF levels and forebrain-specific knockout of BDNF in mice result in deficits in the morphology and function of cortical GABAergic interneurons (11, 12). However, these previous approaches to study the role of BDNF in inhibitory neurons have confounding effects by affecting the development of glutamatergic neurons and other cell types in the brain. To better address this issue, Zheng et al. (13) selectively deleted TrkB from parvalbumin (PV)-positive interneurons and showed that the integration of PV-positive interneurons into the hippocampal microcircuit was impaired and gamma-band rhythmic network activity was disrupted in these mice. However, this mouse model also suffered from severe ataxia and circling behavior, arising from vestibular dysfunction (14), thereby preventing further analyses on potential cognitive and social behavioral changes in these animals.

Here, we have selectively ablated TrkB from a majority of GABAergic interneurons in the cortex and limbic structures (TrkB conditional knockout, otherwise indicated as TrkB cKO) (15). Unexpectedly, these TrkB cKO mice showed disrupted formation of social hierarchies, a fundamental organizing structure in mammalian groups, and exhibited social dominance over control littermates. PV-positive, fast-spiking (FS) inhibitory neurons in TrkB cKO mice exhibited impaired morphological and functional maturation. In addition, these mice showed a disruption in the excitation and inhibition (E/I) balance within the layer 5 (L5) microcircuits of the prelimbic cortex (PrL), an analogous area to dorsolateral prefrontal cortex of primates (16–18). Rectification of the E/I imbalance in the PrL of TrkB cKO mice via optogenetic inhibition of excitatory neuronal activities normalized their social dominance behavior. Taken together, these results demonstrate a role of BDNF/TrkB signaling in cortical GABAergic neurons for social cognition and dominance behavior in mice.

Results

Generation of Corticolimbic GABAergic Neuron-Specific TrkB Knockout Mice. To restrict TrkB ablation to corticolimbic GABAergic interneurons, but not to cerebellar interneurons, we utilized a mouse line in which Cre expression was driven by the protein phosphatase 1 regulatory inhibitor subunit 2 (*Ppp1r2*) gene promoter (*Ppp1r2-Cre*), as described previously (15). To validate the

Significance

Our ability to reason, feel, and socialize relies on the development of a tight balance between inhibition and excitation within cortical circuits. The growth factor BDNF and its receptor TrkB are important for inhibitory neuron development and have been implicated in neuropsychiatric disorders. However, the behavioral consequences of impaired BDNF/TrkB signaling are unknown. Using a transgenic mouse line, we show that mice with deletion of BDNF/TrkB signaling from cortical inhibitory neurons exhibit social dominance and decreased inhibition within the prefrontal cortex, a key region regulating social behavior. Reversal of the network imbalance with optogenetic inhibition could rescue the behavior. Our results reveal a previously uncharacterized role of growth factor signaling within cortical interneurons for the development of social cognition.

Author contributions: S.T. and H.S.J. designed research; S.T. and Y.X. performed research; H.H.Y., A.I.C., and T.W.S. contributed new reagents/analytic tools; S.T., Y.X., and H.S.J. analyzed data; and S.T. and H.S.J. wrote the paper.

The authors declare no conflict of interest.

This article is a PNAS Direct Submission.

[1]To whom correspondence should be addressed. Email: shawn.je@duke-nus.edu.sg.

This article contains supporting information online at www.pnas.org/lookup/suppl/doi:10.1073/pnas.1812083115/-/DCSupplemental.

Published online October 3, 2018.

distribution of Cre-expressing neurons in *Ppp1r2-Cre* mice, we crossed *Ppp1r2-Cre mice* with a loxP-flanked, *Rosa26-tdTomato* ($RTM^{F/F}$) reporter mouse (19) and observed that tdTomato-expressing, Cre-positive neurons were distributed as previously reported (15) (Fig. 1*A*), notably in the cortex and hippocampus. We performed immunostaining experiments in the cortex (specifically prelimbic cortex) of 4-mo-old mice and found that ~95% of tdTomato-positive neurons were positive for GABA (Fig. 1*A*) and these neurons made up ~44% of all GABA-positive cortical neurons (*SI Appendix*, Table S1). The majority of the tdTomato-positive neurons were positive for PV immunostaining (>50%), with the remaining 40% of these neurons made up by other types of GABA-expressing interneurons (*SI Appendix*, Table S1). Next, *Ppp1r2-Cre* mice were crossed with a loxP-flanked TrkB mouse line ($TrkB^{F/F}$) to restrict TrkB deletion to Cre-targeted GABAergic neurons (20–22), and the resulting mice were crossed again with a $RTM^{F/F}$ reporter mouse line (Fig. 1*B*). Using FISH, we detected TrkB mRNA expression in neurons expressing tdTomato mRNA in control mice ($Ppp1r2\text{-}Cre::RTM^{F/F}::TrkB^{WT/WT}$; Ctrl) (Fig. 1*C*). In contrast, TrkB mRNA expression was largely absent in most tdTomato mRNA-expressing neurons in TrkB conditional knockout mice ($Ppp1r2\text{-}Cre::RTM^{F/F}::TrkB^{F/F}$; TrkB cKO) (percentage of TrkB-positive cells over tdTomato-positive cells: Ctrl, 66.81 ± 13.36%; TrkB cKO, 7.323 ± 3.214%; $P < 0.01$), indicating that TrkB gene was successfully ablated in the majority of Cre-targeted, GABA-positive interneurons.

TrkB cKO mice ($Ppp1r2\text{-}Cre::TrkB^{F/F}$ or $Ppp1r2\text{-}Cre::RTM^{F/F}::TrkB^{F/F}$) were viable and fertile. To assess the behavioral changes of TrkB cKO mice, we subjected single-housed TrkB cKO and age-matched control ($TrkB^{F/F}$, Ctrl) male mice (8–20 wk old) to multiple behavioral assays. TrkB cKO mice exhibited no significant difference in body weight, and basic auditory, visual, olfactory, and motor functions (*SI Appendix*, Fig. S1 *A–F* and Table S2). Spontaneous exploration of TrkB cKO mice in an open-field test was normal in terms of the total distance traveled (*SI Appendix*, Fig. S1*G*). An elevated zero maze as well as a light–dark box test (23, 24) revealed that TrkB cKO mice exhibited anxiety-like behaviors, evidenced by a decreased number of transitions in the light–dark box and total time spent in the open arm of an elevated zero maze (*SI Appendix*, Fig. S1 *H* and *I*). Besides anxiety-related behaviors, we did not observe any obvious difference between Ctrl and TrkB cKO mice in other behavioral assays, including spatial working memory (Y-maze), aversive memory (fear conditioning), depressive-like symptoms (tail suspension), sensorimotor gating (prepulse inhibition), and social preference (three-chamber sociability) (*SI Appendix*, Fig. S1 *J–O* and Table S2).

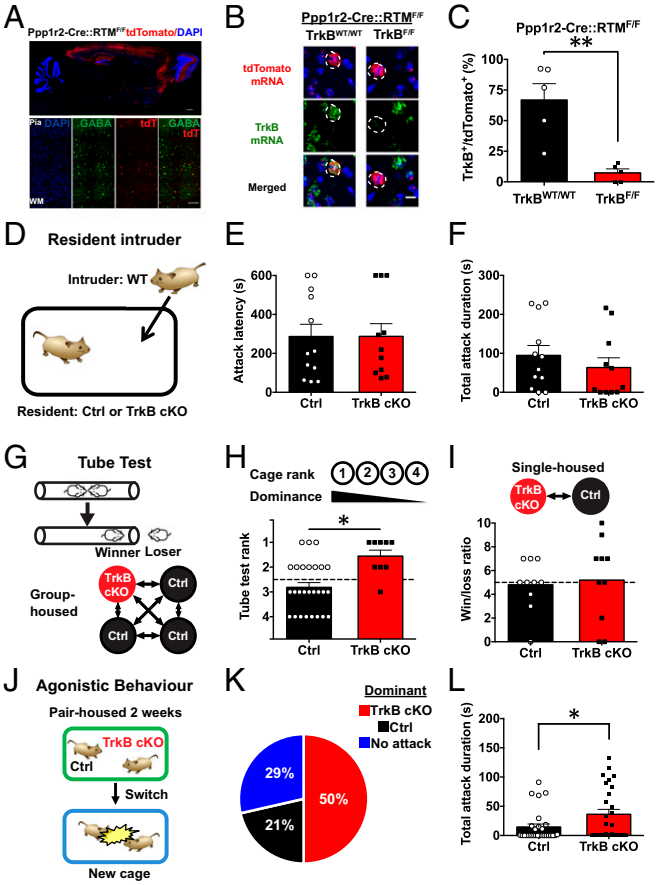

Fig. 1. Corticolimbic GABAergic interneuron-specific ablation of TrkB leads to social dominance in mice. (*A*, *Top*) Overview of a 8-wk-old sagittal brain section from *Ppp1r2-Cre* mice crossed with a *loxP*-flanked $RTM^{F/F}$ reporter mouse line. (Scale bar: 500 μm.) (*A*, *Bottom*) Immunostaining with antibody against GABA in prelimbic cortex ($n = 3$ mice). (Scale bar: 100 μm.) (*B*) Double fluorescence in situ hybridization with probes against tdTomato and TrkB mRNA in cortical sections of 12-wk-old $Ppp1r2\text{-}Cre::RTM^{F/F}::TrkB^{WT/WT}$ and $Ppp1r2\text{-}Cre::RTM^{F/F}::TrkB^{F/F}$ mice. (Scale bar: 10 μm.) The dotted lines indicate representative cell in each group. (*C*) Percentage of tdTomato cells with TrkB mRNA signal in $Ppp1r2\text{-}Cre::RTM^{F/F}::TrkB^{WT/WT}$ and $Ppp1r2\text{-}Cre::RTM^{F/F}::TrkB^{F/F}$ mice ($n = 3$ mice from each group). (*D*) Schematic of resident–intruder test. (*E* and *F*) Attack latency and total duration of attacks between single-housed Ctrl ($TrkB^{F/F}$) and TrkB cKO ($Ppp1r2\text{-}Cre::TrkB^{F/F}$) males in the resident–intruder test (Ctrl, $n = 12$; TrkB cKO, $n = 11$). (*G*) Schematic of the tube test to measure social dominance and social hierarchy. One TrkB cKO and three Ctrl mice were group housed for 2 wk and subjected to round-robin tube test pairing. (*H*) Rankings of each individual mouse on the social hierarchy in nine cages. The dotted line indicates the expected ranking if there was no difference between Ctrl and TrkB cKO mice in terms of social dominance. (*I*) Single-housed Ctrl and TrkB cKO mice with no prior experience with each other were subjected to the tube test and their win/loss ratio was plotted. (*J*) Schematic of the agonistic behavior assay. One Ctrl and one TrkB cKO mouse were pair housed for 2 wk before their home cage was switched for a new one. After the cage switch, the mice were scored on which mice attacked more (dominant) or less (submissive). (*K*) Pie chart of performance in agonistic behavior assay ($n = 28$ pairs). (*L*) Total duration of attack in the agonistic behavioral assay for Ctrl and TrkB cKO mice. Data are presented as means ± SEM. The closed symbols denote individual subjects. Group-housed tube test ranking was assessed by Wilcoxon-signed rank test, others by Student's *t* test. $*P < 0.05$; $**P < 0.01$.

TrkB cKO Mice Displayed Social Dominance Behavior. Intriguingly, despite largely normal behavior of TrkB cKO mice, we observed more frequent fighting in cages housed only with TrkB cKO males. To test whether TrkB cKO mice showed more intermale aggression than Ctrl mice, we performed a resident–intruder test to measure aggressive male behaviors (25–27). Briefly, either Ctrl or TrkB cKO male mouse (12–16 wk old) was singly housed for 2 wk to establish home cage territoriality and was subsequently challenged for 10 min with a wild-type male intruder (Fig. 1*D*). Surprisingly, TrkB cKO males did not show enhanced aggression as measured by the attack latency (Ctrl, 286.5 ± 62.87 s; TrkB cKO, 287.6 ± 65.02 s; $P = 0.99$) and the total duration of biting attacks (Ctrl, 94.79 ± 25.41 s; TrkB cKO, 63.46 ± 25.01 s; $P = 0.39$) (Fig. 1 *E* and *F*).

If not territorial aggression, what did mediate increased fighting incidents among TrkB cKO male mice? Group-housed, male mice tend to fight for social dominance and status within cages (28, 29). Therefore, we hypothesized that increased fighting could be the result of elevated social dominance in TrkB cKO mice. To test this, we performed the tube test, a paradigm to observe and quantify social dominance in laboratory rodents (28, 30) (Fig. 1*G*). In this test, after training to walk through a narrow tube, two mice are placed into opposing ends of a tube.

After a brief interaction period in the middle of the tube, the mouse that consistently forces the opponent to retreat is scored as the more dominant of the pair (Fig. 1*G*) (30). We group-housed one TrkB cKO mouse with three other Ctrl mice (12–16 wk old) for 2 wk and performed the tube test in a pairwise fashion using a round-robin design to determine the rank order (17, 28). After six test sessions over 2 wk, we ranked the four mice in a group with rank 1 being the most dominant and rank 4 being the least dominant (Fig. 1*H*). In support for our hypothesis, we observed that TrkB cKO mice were more dominant in group-housed cages, with the majority occupying either the first or second rank (Fig. 1*H* and Movie S1). The rank distribution for TrkB cKO mice differed significantly from a hypothetical distribution where mice were equally distributed on social rank (median rank of TrkB cKO, 1.0; hypothetical median rank, 2.5; Wilcoxon signed-ranks test, $P = 0.020$) (*SI Appendix*, Table S2). In contrast, when we performed the tube test with single-housed TrkB cKO mice and single-housed Ctrl mice, we could not observe any difference in the win–loss ratios between the two groups (Fig. 1*I*).

As an alternative test for social dominance, we performed an agonistic behavior assay (17). When group-housed mice are placed in a new environment, the dominant male often exhibits agonistic aggression toward cage mates, presumably to claim a new territory (17). We pair-housed one TrkB cKO and one Ctrl mouse for 2 wk and switched their home cage with a new one (Fig. 1*J*). Out of 28 pairs, TrkB cKO mice were approximately twice as likely to be the more dominant aggressor (Fig. 1*K*) and their total attack duration was also higher (Ctrl, 14.57 ± 5.08 s; TrkB cKO, 36.37 ± 8.42 s; $P = 0.031$) (Fig. 1*L*). Taken together, our results suggest that TrkB cKO mice display augmented social dominance behavior.

Interneuron Immaturity and Altered Network Excitatory Synaptic Activity in Layer 5 Neurons Within Prelimbic Cortex of TrkB cKO Mice. Studies have shown that social dominance behavior is mediated by microcircuits within the medial prefrontal cortex (mPFC), which corresponds to the anterior cingulate cortex (ACC), prelimbic (PrL), and infralimbic (IL) areas in rodents (31–34). In particular, the PrL area in mice is specifically activated upon social contact (35), and selective manipulation of excitatory synaptic transmission within the PrL can alter the formation of social dominance hierarchy (17). First, we examined the intrinsic properties of tdTomato-positive interneurons within the PrL from Ctrl and TrkB cKO mice (Fig. 2*A*). Due to the heterogeneity of GABAergic interneurons, we restricted our analysis to FS, PV- and tdTomato-positive interneurons, which play important modulatory roles in cortical microcircuits (Fig. 2*B*) (36–39). Retrospective immunolabeling showed that the recorded interneurons with FS firing patterns were indeed positive for PV immunostaining (Fig. 2*B*). Interestingly, upon a series of current injections, we found that tdTomato-positive, FS interneurons (FSINs) of TrkB cKO mice exhibited functional differences. FSINs from TrkB cKO mice showed (*i*) increased spike frequency adaptation [two-way ANOVA, interaction: $F_{(6,126)} = 2.927$, $P = 0.0105$; main effect of interspike interval: $F_{(6,126)} = 47.30$, $P < 0.0001$; main effect of genotype: $F_{(1,21)} = 5.079$, $P = 0.0350$; Fig. 2 *C* and *D*], (*ii*) wider action potential half-width (Ctrl, 0.423 ± 0.017 ms; TrkB cKO, 0.504 ± 0.019 ms; $P = 0.0056$; Fig. 2 *E* and *F*), and (*iii*) longer membrane time constants (Ctrl, 6.927 ± 0.3190 ms; TrkB cKO, 10.58 ± 0.5877 ms; $P < 0.0001$; Fig. 2 *G* and *H*). In addition, other intrinsic properties of FSINs were significantly different in TrkB cKO mice, including the input resistance, action potential amplitude, and action potential threshold, but we could not observe any significant change in the resting membrane potential (*SI Appendix*, Fig. S2). Given that FSINs display a unique set of electrophysiological properties upon developmental maturation

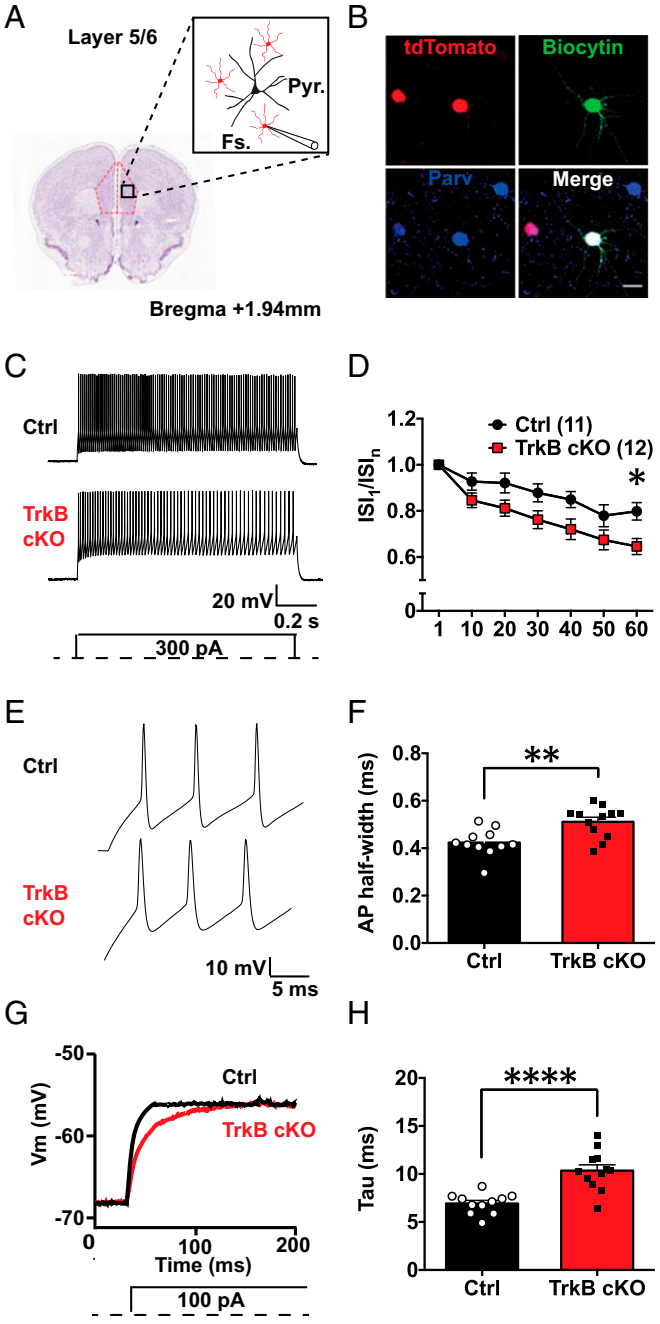

Fig. 2. TrkB cKO FSINs in prelimbic cortex are functionally impaired. (*A*) Schematic diagram of the mouse mPFC, as outlined by the red dashed lines. The black box indicates close-up of the neurons that were patched. We performed whole-cell patch-clamp recordings from L5/6 tdTomato-labeled FSINs of *Ppp1r2-Cre::RTM$^{F/F}$::TrkB$^{WT/WT}$* (Ctrl) and *Ppp1r2-Cre::RTM$^{F/F}$::TrkB$^{F/F}$* (TrkB cKO) mice. Fs., FSINs; Pyr, pyramidal neuron. (*B*) A L5 tdTomato (red)-labeled FSIN that was filled with biocytin (green) and subsequently confirmed to express parvalbumin (parv) (blue). (Scale bar: 20 μm.) (*C*) Representative trace of action potential trains elicited by depolarizing current injection (300 pA). (*D*) Frequency adaptation as illustrated by the ratio of the first interspike interval (ISI$_1$) over the *n*th interspike interval (ISI$_n$). (*E*) Representative trace of action potentials evoked by a depolarizing current injection in L5/6 tdTomato FSINs of Ctrl and TrkB cKO mice (50 pA above spiking threshold). (*F*) Bar plot of action potential half-width. (*G*) Representative trace of membrane potential deflection evoked by a depolarizing current injection (100 pA). (*H*) Bar plot of membrane time constant. Data are presented as means ± SEM. Ctrl, $n = 11$ neurons; TrkB cKO, $n = 12$ neurons. $n = 4$–5 mice per group. The closed symbols denote individual neurons. Adaptation ratio was assessed by one-way ANOVA, others by Student's *t* test. *$P < 0.05$; **$P < 0.01$; ****$P < 0.0001$.

(40, 41), our data suggest that FSINs of TrkB cKO exhibited functional immaturity.

Previously, it has been shown that immature inhibitory neuron function and synapse formation may affect spontaneous synaptic activities of nearby pyramidal neurons within the same microcircuits due to impaired network inhibition (6, 13). In the mPFC, top–down information is transmitted via pathways from layer 2/3 pyramidal neurons to pyramidal neurons in L5, which is a major corticofugal output layer of the PFC network (42). Therefore, we measured the spontaneous excitatory postsynaptic currents (sEPSCs) of L5 pyramidal neurons in PrL of Ctrl and TrkB cKO mice (Fig. 3*A*). Intriguingly, we observed an increase in the frequency of sEPSCs (Ctrl, 4.33 ± 0.51 Hz; TrkB cKO, 7.43 ± 1.34 Hz; $P = 0.038$), but not in the amplitudes (Ctrl, 18.31 ± 0.63 pA; TrkB cKO, 18.60 ± 0.80 pA; $P = 0.78$) (Fig. 3 *A–C*), suggesting increased spontaneous excitatory synaptic transmission in TrkB cKO cortex. We also measured spontaneous miniature inhibitory postsynaptic currents (mIPSCs), from L5 pyramidal neurons of Ctrl and TrkB cKO mice. Intriguingly, we observed a significant reduction in the frequency of mIPSCs (Ctrl, 16.37 ± 1.68 Hz; TrkB cKO, 11.57 ± 1.11 Hz, $P = 0.029$), with no change in the amplitude (Ctrl, 37.05 ± 2.71 pA; TrkB cKO, 34.20 ± pA, $P = 0.48$) (Fig. 3 *D–F*), indicating the reduced inhibitory synaptic inputs/synapses onto excitatory neurons in TrkB cKO mice. Three-dimensional morphometric analyses of biocytin-labeled and recorded interneurons of Ctrl and TrkB cKO mice revealed reduced neurite arborization [two-way ANOVA, interaction, $F_{(36,1008)} = 2.713$, $P < 0.0001$; main effect of distance from soma, $F_{(36,1008)} = 199.1$, $P < 0.0001$; main effect of genotype, $F_{(1,28)} = 3.096$, $P = 0.0894$] and reduced total number of neurites (Ctrl, 31.37 ± 1.90; TrkB cKO, 25.36 ± 0.77, $P = 0.0273$) (Fig. 3 *G–I*) in TrkB cKO interneurons. Taken together, the lack of BDNF/TrkB signaling in GABAergic FSINs disrupted the functional and morphological maturation of inhibitory interneurons, which subsequently impaired inhibitory modulation within L5 cortical microcircuits of the PrL in TrkB cKO mice.

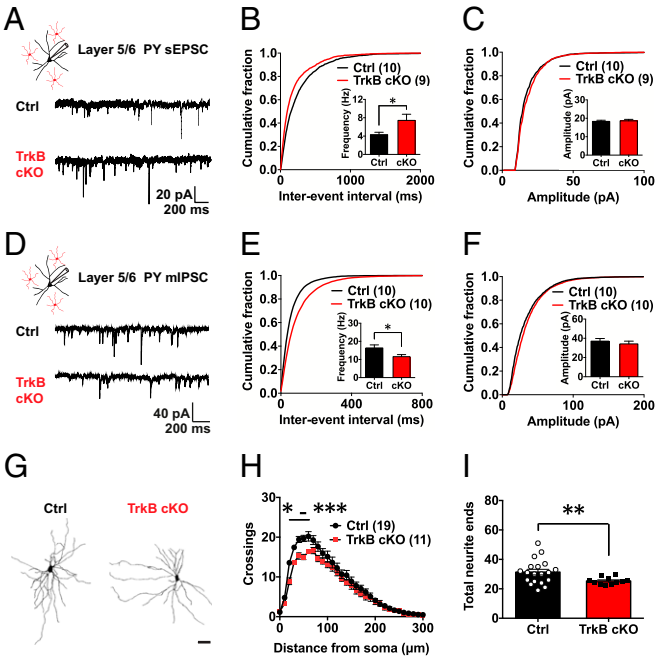

Fig. 3. Reduced inhibitory inputs to excitatory neurons and enhanced excitatory basal transmission in prelimbic cortex of TrkB cKO mice. (*A*) Sample traces of spontaneous excitatory postsynaptic currents (sEPSCs) recorded from L5/6 pyramidal neurons of Ctrl vs. TrkB cKO mice. (*B* and *C*) Cumulative probability distribution and bar plot of sEPSC (*B*) frequency and (*C*) amplitude recorded from L5/6 pyramidal neurons of Ctrl vs. TrkB cKO mice. (*D*) Sample traces of spontaneous miniature inhibitory postsynaptic currents (mIPSCs) recorded from L5/6 pyramidal neurons of Ctrl vs. TrkB cKO mice. (*E* and *F*) Cumulative probability distribution and bar plot of mIPSC (*E*) frequency and (*F*) amplitude recorded from L5/6 pyramidal neurons of Ctrl vs. TrkB cKO mice. (*G*) Representative traces of biocytin-filled Ctrl vs. TrkB cKO interneurons. (Scale bar: 50 μm.) (*H*) Sholl analysis of 3D-reconstructed Ctrl vs. TrkB cKO interneurons. (*I*) Bar plot of total number of neurites ends. Data are presented as means ± SEM; $n = 4–5$ mice per group; Student's *t* test, $^*P < 0.05$; $^{**}P < 0.01$; $^{***}P < 0.001$.

Optogenetic Silencing of Excitatory Neurons Within Prelimbic Cortex Normalized Social Dominance Behavior in TrkB cKO Mice. It remains unclear whether the imbalance in network activities within prelimbic microcircuits caused social dominance behavior in TrkB cKO mice. To test this, we bilaterally injected adeno-associated virus (AAV) containing double-floxed, light-sensitive excitatory opsin, channelrhodopsin-2 (ChR2) (43), into the PrL of TrkB cKO mice to limit ChR2 expression to only Cre-expressing interneurons of TrkB cKO mice. However, we found that the acute activation of inhibitory neurons during tube test could not reverse the social dominance behavior of TrkB cKO mice (*SI Appendix*, Fig. S3).

Instead, we tested whether the transient inhibition of excitatory neurons in the PrL of TrkB cKO mice could reverse social dominance behaviors. We bilaterally injected AAV, containing the light-sensitive inhibitory opsin archaerhodopsin (eArch) under the control of CAMKIIα promoter (CAMKII-eArch3.0-EYFP) (44), which restricted expression to excitatory pyramidal neurons, into the PrL of TrkB cKO mice (Fig. 4 *A* and *B* and *SI Appendix*, Fig. S4 *A* and *B*). Light activation of eArch-expressing neurons in acute brain slices of the PrL acutely silenced evoked action potentials (light off, 9.3 ± 1.7 Hz; light on, 0 ± 0.0 Hz; $P = 0.005$; Fig. 4 *C* and *D*). Next, we repeated the tube test in group-housed TrkB cKO mice injected with CAMKII-eArch and Ctrl mice with or without light stimulation (Fig. 4 *E* and *F* and *SI Appendix*, Fig. S4*C*). Intriguingly, optogenetic inhibition of excitatory neurons during the tube test normalized social dominance behaviors in TrkB cKO mice, indicated by lower rank in the tube test (tube test rank: light off, 1.143; light on, 2.214, $P = 0.032$), which rebounded when light stimulation was not delivered (light on, 2.214; light off, 1.286; $P = 0.032$; Fig. 4 *E* and *F* and Movie S2). Light stimulation of CAMKII-EGFP–injected TrkB cKO mice did not trigger any change in the tube test rank (Fig. 4*F*). Moreover, we did not observe any alteration in light-stimulated TrkB cKO mice in general locomotor activity in the open field test (*SI Appendix*, Fig. S4*D*).

Taken together, our results suggest that the acute inhibition of excitatory neuronal activities in the PrL of TrkB cKO mice is sufficient to reverse social dominance behavior, indicating that defective inhibitory modulation in the PrL microcircuits of TrkB cKO might result in social dominant behaviors by triggering E/I network imbalance.

Discussion

Here, we demonstrated that postnatal ablation of BDNF/TrkB signaling from corticolimbic GABAergic interneurons resulted in social dominance behavior. These behavioral changes were potentially due to developmental immaturity of GABAergic interneurons. This consequently resulted in decreased inhibitory modulation and up-regulated excitatory synaptic transmission within the L5 of the mPFC microcircuits. Abnormal behavior of TrkB cKO mice were ameliorated by reducing the activity of excitatory neurons in the mPFC via optogenetic inhibition, indicating that network E/I balance might be crucial for social cognition and the regulation of dominance hierarchy formation.

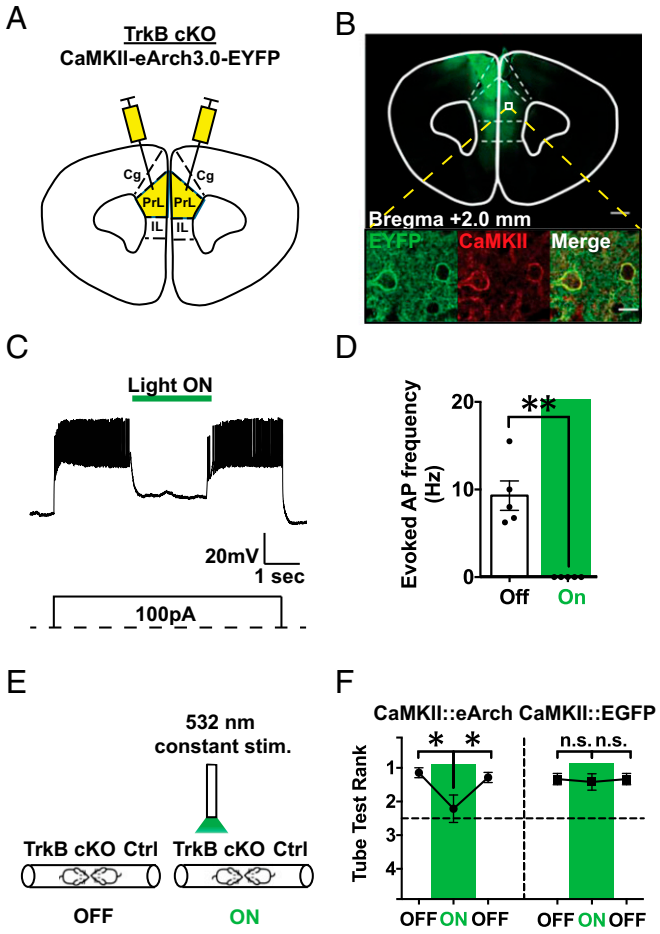

Fig. 4. Optogenetic silencing of PrL normalizes social dominance in TrkB cKO mice. (*A*) TrkB cKO mice were bilaterally injected with AAV-CAMKII-eArch-EYFP into the prelimbic area (PrL). Cg, cingulate cortex; IL, infralimbic cortex. (*B*) Representative image of viral transduction and close-up showing immunostaining of dense EYFP-positive neuropil and membrane labeling of individual CaMKII-positive neurons. (Scale bars: *Top*, 500 μm; *Bottom*, 20 μm) (*C*) Green light illumination silenced current injection evoked action potentials in whole-cell patch clamp of L5 pyramidal neurons labeled with eArch. (*D*) Quantification of change in firing rate with green light illumination ($n = 5$ neurons from three mice) (current injection, 100–300 pA). (*E*) Schematic of tube test with green light stimulation to optogenetically inhibit the PrL. (*F*) Plot of change in tube test rank as a result of optogenetic inhibition. As a control, a separate group of TrkB cKO mice were injected with CAMKII::EYFP and underwent similar stimulation. The closed symbols denote individual neurons in *D* and individual subjects in *F*. Data are presented as means ± SEM. CaMKII::eArch, $n = 7$; CaMKII::EGFP, $n = 6$; Student's *t* test, $^{*}P < 0.05$; $^{**}P < 0.01$.

Role of BDNF/TrkB Signaling in mPFC in Regulation of Social Dominance. Reduced BDNF level and its signaling in the brain have been linked to aggressive and dominant behavior. The BDNF Val66Met ($BDNF^{Met}$) polymorphism, which leads to reduced activity-dependent BDNF secretion in the brain (45), is associated with aggressive behaviors in humans (46, 47). In animals, $BDNF^{+/-}$, Nestin-Cre::$BDNF^{F/F}$, CaMKII-Cre::$BDNF^{F/F}$, KA1-Cre::$BDNF^{F/F}$, and $BDNF^{Met/Met}$ male mice all showed enhanced aggression (48–51). While these studies indicated strong association between attenuated BDNF level in the brain and aggressive animal behavior, the presence of other confounding behavioral phenotypes (e.g., depression- and anxiety-like behaviors) as well as the requirement for BDNF signaling in multiple subtypes of neurons (glutamatergic, GABAergic, cholinergic, and serotonergic neurons) (4, 12, 48, 52) made it difficult to pinpoint which neuronal subtypes and which neuronal circuits were linked to BDNF-dependent, aggressive behavior.

Previous studies have directly shown that mPFC microcircuits play important role for social dominance and aggression behavior in animals. For example, neurons within mPFC are directly activated by social contact (35), and mPFC lesions can trigger aggressive behaviors in both rats and humans (53, 54). More recently, it was reported that bidirectional modulation of synaptic strength in mPFC (17) and optogenetic stimulation/chemogenetic inhibition of mPFC excitatory neurons was necessary and sufficient to modulate social rank in mice (55).

Intriguingly, our TrkB cKO mice, in which BDNF/TrkB signaling was attenuated postnatally only in corticolimbic GABAergic interneurons, exhibit social dominance, without affecting other types of aggressive behaviors (Fig. 1 *D–H*) (25). More interestingly, singly housed TrkB cKO did not show social dominance, indicating that TrkB cKO were not intrinsically aggressive and that social experience was necessary (Fig. 1*I*).

While our data suggest that artificially manipulating BDNF/TrkB signaling in corticolimbic GABAergic interneurons can modulate social dominance behavior, it is still unclear whether this is relevant for endogenous BDNF/TrkB. Previous studies that have looked at environmental manipulations that modulate BDNF suggest that this is possible. Interestingly, mice reared in communal nests have increased cortical and hippocampal BDNF levels and adopted social status quicker than control mice raised in single nests (56, 57). In addition, these mice showed higher levels of postfight reconciliatory behaviors, indicating potential role of BDNF modulation in the development or stabilization of social cognition in mice. It will be exciting to test whether naturally dominant and submissive mice have differential levels of BDNF/TrkB signaling in corticolimbic interneurons.

Role of BDNF/TrkB Signaling in Development and Maturation of GABAergic Interneurons and Network E/I Balance in the Local Cortical Neuronal Network. Genetic ablation of TrkB in early postnatal interneurons resulted in multiple aberrant changes in the intrinsic properties of FSINs (Fig. 2), which prevented them from responding accurately to incoming synaptic inputs (58, 59). These changes could be caused by disrupted expression of ion channels (40, 41). For example, members of the Kv3 subfamily (Kv3.1b, Kv3.2) of voltage-gated potassium channels are specifically enriched in neocortical interneurons (60) and contribute to fast repolarization and high-frequency firing. Further studies could investigate these possible candidates. We cannot rule out the possibility that other classes of interneurons were also affected in our TrkB cKO mice, but we did not include analyses of these non-FS interneurons due to their low numbers and heterogeneity (61). Further studies using in vivo calcium imaging and multielectrode recordings will help us to delineate network-level changes in inhibitory and excitatory activity in TrkB cKO mice during their social aggressive behaviors (62, 63).

Several converging lines of evidence suggest that impaired inhibitory modulation by PV-positive FSINs was the cause of enhanced excitatory spontaneous synaptic transmission within the PFC. First, PV-positive neurons were the majority of targeted neurons in the PFC of the *Ppp1r2-Cre* mice line (*SI Appendix*, Table S1). Second, among cortical GABAergic neurons, the level of TrkB expression is the highest in PV-positive neurons, followed by somatostatin (SST)-positive neurons (64), suggesting ontological BDNF dependence of PV-positive neurons. In support for this, in BDNF-overexpressed mice, cortical PV expression is accelerated (4), whereas the loss of activity-dependent BDNF expression leads to reduced number of PV-positive neurons in the mPFC (65). Likewise, in BDNF-KO mice, PV-positive FSINs show delayed electrophysiological maturation, which is similar to our results (66). Third, within the mPFC, perisomatic targeting PV-positive FSINs mediate fast

and powerful inhibition of excitatory neurons. However, dendritic targeting SST-positive INs mediate weak and variable inhibition (67). Last, previous studies with TrkB cKO using PV-cre transgenic mice indicated reduced inhibitory synaptic connections onto excitatory neurons and subsequently resulted in increased excitatory output in the cortical microcircuits (13, 68). Taken together, these findings suggest that TrkB disruption in PV-positive neurons resulted in increased excitatory activity and network-level imbalance in our TrkB cKO.

Intriguingly, our results are slightly different from a previous study that reported an increase in the amplitude, but not the frequency, of miniature EPSCs in naturally dominant mice compared with their submissive cage mates (17). Compared with our genetic manipulation, the underlying mechanism of social dominance in animals of Wang et al. could be either epigenetic or individual differences that would lead to different synaptic changes (69). In addition, Wang et al. did not investigate the involvement of GABAergic neurons and inhibitory modulation in their social behavior paradigms. The reversal of social dominance in TrkB cKO by optogenetic inhibition of mPFC excitatory neurons concurs with a similar optogenetic study by Zhou et al. (55). In summary, our studies are concurrent with the notion that network activity and E/I balance within mPFC microcircuits influences social dominance behavior in mice.

Although we did not observe significant difference in social dominance behavior of TrkB cKO mice when we artificially manipulated PV interneurons (*SI Appendix*, Fig. S3), this could be due to two reasons. One, the artificial chronic stimulation could not mimic or compensate for the developmental change in PV interneurons in TrkB conditional mice. The other reason could be that we did not recruit and activate enough numbers of PV interneurons to elicit a behavioral effect.

Taken together, we show that the postnatal ablation of BDNF/TrkB signaling in corticolimbic GABAergic interneurons results in social dominance by the disruption of the E/I balance in mPFC microcircuits. Our genetic model could be useful to dissociate and dissect underlying molecular and cellular mechanisms of aggressive behaviors and social cognition in mice.

Materials and Methods

Detailed experimental procedures are provided in *SI Appendix, SI Materials and Methods*.

Husbandry and Animals. *Ppp1r2-Cre* mice were obtained from Dr. Kazu Nakazawa, Southern Research, Birmingham, AL (15), $TrkB^{F/F}$ mice from Dr. Luis Parada, Memorial Sloan Kettering Cancer Center, New York (22), and $RTM^{F/F}$ mice from The Jackson Laboratory (19). Animals were housed in a specific-pathogen–free facility maintained below 22 °C, 55% humidity, with food and water provided ad libitum, on a 12-h light cycle (lights on at 0700 h). With the exception of tube test for social dominance, adult males (8–20 wk) were singled-housed for the other behavioral tests. All procedures to maintain and use these mice were approved by the Institutional Animal Care and Use Committee for Duke–National University of Singapore Medical School (IACUC 2010/SHS/590 and 2014/SHS/999).

Double Fluorescence in Situ Hybridization. In situ hybridization was performed using RNA probes targeting the TrkB kinase domain (70) and tdTomato (Allen Mouse Brain Atlas probes; Riboprobe ID, RP_099999_01_A05) (71). The in situ hybridization procedure can be found in *SI Appendix, SI Materials and Methods*.

Resident–Intruder Test. For the resident–intruder test, mice were single-housed for at least 1 wk before testing to establish territoriality. A wild-type C57/BL6 "intruder" (weighing at least 10% less than the resident and group-housed before the test) was introduced to the resident's home cage for a total duration of 10 min.

Tube Test. During the test trial, two mice were introduced into either entrance of the tube, where both mice would meet at the center of the tube. The trial was terminated when either mouse was pushed out, or left the tube voluntarily, or if both mice still remained after 2 min. For the group social dominance tube test, one TrkB cKO mouse and three Ctrl mice were group housed for 2 wk before testing. The mice were ranked overall based on the number of winning bouts after six repeated sessions over 2 wk. For single-housed social dominance tube test, mice were single-housed for at least 1 wk before testing. Each mouse was paired against five opponents of the opposite genotype and around the same weight (~2 g).

Agonistic Behavior Assay. For the agonistic behavioral assay, one TrkB cKO mouse and one Ctrl mouse were paired-housed for 2 wk. After that, they were switched over to a new cage and their interactions were videotaped.

Slice Electrophysiology. Slices containing mPFC were prepared from 13- to 18-wk-old C57/BL6 male mice, and acute slice recording was performed as previously described (6). Pyramidal neurons in the L4–5 of mPFC were identified by their differential interference contrast morphology and electrophysiological properties (spike firing pattern). TrkB cKO and Ctrl FSINs were identified by tdTomato expression and electrophysiological properties. For anatomical reconstruction, the internal solution was filled with 0.3% biocytin (Sigma) during whole-cell recordings. Additional details on solutions and analysis of parameters can be found in *SI Appendix, SI Materials and Methods*.

Stereotaxic Surgery and Optogenetic Manipulation. Stereotaxic surgery, virus injections, and fiber-optic implants was performed on 3- to 4-mo-old TrkB cKO or Ctrl mice as previous described (72). Injection coordinates for the PrL were +2.0 mm anteroposterior, ±0.8 mm mediolateral, and −1.8 mm dorsoventral (at a 15° angle). A volume of 0.5 uL of either AAV5-CaMKIIa-eArch3.0-EYFP or AAV5-CAMKIIa-EGFP virus (~2.5×10^{12} infectious units/mL; University of North Carolina Vector Core) was infused into the site at 100 nL/min. Mice were group-housed and allowed to recover at least 2 wk before behavioral testing. Before stimulation, the output was adjusted such that 10 mW of illumination was delivered from the fiber optic tip. Additional details can be found in *SI Appendix, SI Materials and Methods*.

Statistical Analyses and Graphs. Data were analyzed and plotted using GraphPad Prism (GraphPad Software) and presented as means ± SEM. Data were analyzed using either two-tailed paired or unpaired *t* test, or by one-way ANOVA followed by Tukey's post hoc test. Outliers were identified by the Grubbs' outlier test (73) and were excluded from analysis.

ACKNOWLEDGMENTS. We thank Rahul Jawa, Hasini Ganegala, and Younghwan Lee for colony maintenance and Dr. Wong Peiyan for assistance with behavioral experiments. We also thank Ms. Norliyana Binte Zainolabidin for assistance with in situ hybridization experiments and Dr. Mark Rossi for help with optogenetic experiments. We thank Drs. Carlos Ibanez and Chul-Hoon Kim for their critical comments on the manuscript. This work was supported by the Singapore Ministry of Education (MOE) Academic Research Fund [MOE2014-T2-2-071 (to H.S.J.)], National Medical Research Council Collaborative Research Grants NMRC/CBRG/0075/2014 (to H.S.J. and A.I.C.) and NMRC/OFIRG/0050/2017 (to H.S.J.), an A*Star Translational Collaborative Research Partnership Grant [13/1/96/688 (to H.S.J.)], a Duke–National University of Singapore (NUS) Signature Research Program Block Grant (to H.S.J.), NIH Grant R01MH112883 (to H.H.Y.), and an NUS Graduate School for Integrative Sciences and Engineering Scholarship (to S.T.).

1. Horch HW, Katz LC (2002) BDNF release from single cells elicits local dendritic growth in nearby neurons. *Nat Neurosci* 5:1177–1184.
2. Marshall CJ (1995) Specificity of receptor tyrosine kinase signaling: Transient versus sustained extracellular signal-regulated kinase activation. *Cell* 80:179–185.
3. Park H, Poo M-M (2013) Neurotrophin regulation of neural circuit development and function. *Nat Rev Neurosci* 14:7–23.
4. Huang ZJ, et al. (1999) BDNF regulates the maturation of inhibition and the critical period of plasticity in mouse visual cortex. *Cell* 98:739–755.
5. Kohara K, et al. (2007) A local reduction in cortical GABAergic synapses after a loss of endogenous brain-derived neurotrophic factor, as revealed by single-cell gene knockout method. *J Neurosci* 27:7234–7244.
6. Yuan Q, et al. (2016) Regulation of brain-derived neurotrophic factor exocytosis and gamma-aminobutyric acidergic interneuron synapse by the schizophrenia susceptibility gene dysbindin-1. *Biol Psychiatry* 80:312–322.
7. Sánchez-Huertas C, Rico B (2011) CREB-dependent regulation of GAD65 transcription by BDNF/TrkB in cortical interneurons. *Cereb Cortex* 21:777–788.
8. Kohara K, et al. (2003) Inhibitory but not excitatory cortical neurons require presynaptic brain-derived neurotrophic factor for dendritic development, as revealed by chimera cell culture. *J Neurosci* 23:6123–6131.
9. Yamada MK, et al. (2002) Brain-derived neurotrophic factor promotes the maturation of GABAergic mechanisms in cultured hippocampal neurons. *J Neurosci* 22:7580–7585.

10. Wardle RA, Poo M-M (2003) Brain-derived neurotrophic factor modulation of GABAergic synapses by postsynaptic regulation of chloride transport. *J Neurosci* 23:8722–8732.
11. Abidin I, Eysel UT, Lessmann V, Mittmann T (2008) Impaired GABAergic inhibition in the visual cortex of brain-derived neurotrophic factor heterozygous knockout mice. *J Physiol* 586:1885–1901.
12. Gorski JA, Zeiler SR, Tamowski S, Jones KR (2003) Brain-derived neurotrophic factor is required for the maintenance of cortical dendrites. *J Neurosci* 23:6856–6865.
13. Zheng K, et al. (2011) TrkB signaling in parvalbumin-positive interneurons is critical for gamma-band network synchronization in hippocampus. *Proc Natl Acad Sci USA* 108:17201–17206.
14. Lucas EK, Jegarl A, Clem RL (2014) Mice lacking TrkB in parvalbumin-positive cells exhibit sexually dimorphic behavioral phenotypes. *Behav Brain Res* 274:219–225.
15. Belforte JE, et al. (2010) Postnatal NMDA receptor ablation in corticolimbic interneurons confers schizophrenia-like phenotypes. *Nat Neurosci* 13:76–83.
16. Yizhar O, et al. (2011) Neocortical excitation/inhibition balance in information processing and social dysfunction. *Nature* 477:171–178.
17. Wang F, et al. (2011) Bidirectional control of social hierarchy by synaptic efficacy in medial prefrontal cortex. *Science* 334:693–697.
18. Takahashi A, Nagayasu K, Nishitani N, Kaneko S, Koide T (2014) Control of intermale aggression by medial prefrontal cortex activation in the mouse. *PLoS One* 9:e94657.
19. Madisen L, et al. (2010) A robust and high-throughput Cre reporting and characterization system for the whole mouse brain. *Nat Neurosci* 13:133–140.
20. He X-P, et al. (2004) Conditional deletion of TrkB but not BDNF prevents epileptogenesis in the kindling model. *Neuron* 43:31–42.
21. Li Y, et al. (2012) Conditional ablation of brain-derived neurotrophic factor-TrkB signaling impairs striatal neuron development. *Proc Natl Acad Sci USA* 109: 15491–15496.
22. Luikart BW, Nef S, Shipman T, Parada LF (2003) In vivo role of truncated trkb receptors during sensory ganglion neurogenesis. *Neuroscience* 117:847–858.
23. Bourin M, Hascoët M (2003) The mouse light/dark box test. *Eur J Pharmacol* 463: 55–65.
24. Shepherd JK, Grewal SS, Fletcher A, Bill DJ, Dourish CT (1994) Behavioural and pharmacological characterisation of the elevated "zero-maze" as an animal model of anxiety. *Psychopharmacology (Berl)* 116:56–64.
25. Miczek KA, Maxson SC, Fish EW, Faccidomo S (2001) Aggressive behavioral phenotypes in mice. *Behav Brain Res* 125:167–181.
26. Nelson RJ, Chiavegatto S (2000) Aggression in knockout mice. *ILAR J* 41:153–162.
27. Koolhaas JM, et al. (2013) The resident-intruder paradigm: A standardized test for aggression, violence and social stress. *J Vis Exp*, e4367.
28. van den Berg WE, Lamballais S, Kushner SA (2015) Sex-specific mechanism of social hierarchy in mice. *Neuropsychopharmacology* 40:1364–1372.
29. Van Loo PL, Mol JA, Koolhaas JM, Van Zutphen BF, Baumans V (2001) Modulation of aggression in male mice: Influence of group size and cage size. *Physiol Behav* 72: 675–683.
30. Lindzey G, Winston H, Manosevitz M (1961) Social dominance in inbred mouse strains. *Nature* 191:474–476.
31. Freeman JB, Rule NO, Adams RB, Jr, Ambady N (2009) Culture shapes a mesolimbic response to signals of dominance and subordination that associates with behavior. *Neuroimage* 47:353–359.
32. Holson RR (1986) Mesial prefrontal cortical lesions and timidity in rats. III. Behavior in a semi-natural environment. *Physiol Behav* 37:239–247.
33. Fujii N, Hihara S, Nagasaka Y, Iriki A (2009) Social state representation in prefrontal cortex. *Soc Neurosci* 4:73–84.
34. Zink CF, et al. (2008) Know your place: Neural processing of social hierarchy in humans. *Neuron* 58:273–283.
35. Avale ME, et al. (2011) Prefrontal nicotinic receptors control novel social interaction between mice. *FASEB J* 25:2145–2155.
36. Galarreta M, Hestrin S (1999) A network of fast-spiking cells in the neocortex connected by electrical synapses. *Nature* 402:72–75.
37. Kawaguchi Y, Katsumaru H, Kosaka T, Heizmann CW, Hama K (1987) Fast spiking cells in rat hippocampus (CA1 region) contain the calcium-binding protein parvalbumin. *Brain Res* 416:369–374.
38. Cunningham MO, et al. (2004) A role for fast rhythmic bursting neurons in cortical gamma oscillations in vitro. *Proc Natl Acad Sci USA* 101:7152–7157.
39. Hu H, Gan J, Jonas P (2014) Interneurons. Fast-spiking, parvalbumin^{+} GABAergic interneurons: From cellular design to microcircuit function. *Science* 345:1255263.
40. Goldberg EM, et al. (2011) Rapid developmental maturation of neocortical FS cell intrinsic excitability. *Cereb Cortex* 21:666–682.
41. Okaty BW, Miller MN, Sugino K, Hempel CM, Nelson SB (2009) Transcriptional and electrophysiological maturation of neocortical fast-spiking GABAergic interneurons. *J Neurosci* 29:7040–7052.
42. Molyneaux BJ, Arlotta P, Menezes JRL, Macklis JD (2007) Neuronal subtype specification in the cerebral cortex. *Nat Rev Neurosci* 8:427–437.
43. Cardin JA, et al. (2010) Targeted optogenetic stimulation and recording of neurons in vivo using cell-type-specific expression of channelrhodopsin-2. *Nat Protoc* 5:247–254.
44. Mattis J, et al. (2011) Principles for applying optogenetic tools derived from direct comparative analysis of microbial opsins. *Nat Methods* 9:159–172.
45. Egan MF, et al. (2003) The BDNF val66met polymorphism affects activity-dependent secretion of BDNF and human memory and hippocampal function. *Cell* 112:257–269.
46. Spalletta G, et al. (2010) BDNF Val66Met polymorphism is associated with aggressive behavior in schizophrenia. *Eur Psychiatry* 25:311–313.
47. Kretschmer T, Vitaro F, Barker ED (2014) The association between peer and own aggression is moderated by the *BDNF* val-met polymorphism. *J Res Adolesc* 24: 177–185.
48. Lyons WE, et al. (1999) Brain-derived neurotrophic factor-deficient mice develop aggressiveness and hyperphagia in conjunction with brain serotonergic abnormalities. *Proc Natl Acad Sci USA* 96:15239–15244.
49. Chan JP, Unger TJ, Byrnes J, Rios M (2006) Examination of behavioral deficits triggered by targeting Bdnf in fetal or postnatal brains of mice. *Neuroscience* 142:49–58.
50. Ito W, Chehab M, Thakur S, Li J, Morozov A (2011) BDNF-restricted knockout mice as an animal model for aggression. *Genes Brain Behav* 10:365–374.
51. Chen Z-Y, et al. (2006) Genetic variant BDNF (Val66Met) polymorphism alters anxiety-related behavior. *Science* 314:140–143.
52. Morse JK, et al. (1993) Brain-derived neurotrophic factor (BDNF) prevents the degeneration of medial septal cholinergic neurons following fimbria transection. *J Neurosci* 13:4146–4156.
53. de Bruin JP, van Oyen HG, Van de Poll N (1983) Behavioural changes following lesions of the orbital prefrontal cortex in male rats. *Behav Brain Res* 10:209–232.
54. Grafman J, et al. (1996) Frontal lobe injuries, violence, and aggression: A report of the Vietnam Head Injury Study. *Neurology* 46:1231–1238.
55. Zhou T, et al. (2017) History of winning remodels thalamo-PFC circuit to reinforce social dominance. *Science* 357:162–168.
56. Branchi I, et al. (2013) Early interactions with mother and peers independently build adult social skills and shape BDNF and oxytocin receptor brain levels. *Psychoneuroendocrinology* 38:522–532.
57. Branchi I, et al. (2006) Early social enrichment shapes social behavior and nerve growth factor and brain-derived neurotrophic factor levels in the adult mouse brain. *Biol Psychiatry* 60:690–696.
58. Jonas P, Bischofberger J, Fricker D, Miles R (2004) Interneuron diversity series: Fast in, fast out—temporal and spatial signal processing in hippocampal interneurons. *Trends Neurosci* 27:30–40.
59. Kawaguchi Y (1995) Physiological subgroups of nonpyramidal cells with specific morphological characteristics in layer II/III of rat frontal cortex. *J Neurosci* 15: 2638–2655.
60. Chow A, et al. (1999) K^{+} channel expression distinguishes subpopulations of parvalbumin- and somatostatin-containing neocortical interneurons. *J Neurosci* 19: 9332–9345.
61. Cauli B, et al. (2000) Classification of fusiform neocortical interneurons based on unsupervised clustering. *Proc Natl Acad Sci USA* 97:6144–6149.
62. Lin D, et al. (2011) Functional identification of an aggression locus in the mouse hypothalamus. *Nature* 470:221–226.
63. Packer AM, Russell LE, Dalgleish HWP, Häusser M (2015) Simultaneous all-optical manipulation and recording of neural circuit activity with cellular resolution in vivo. *Nat Methods* 12:140–146.
64. Gorba T, Wahle P (1999) Expression of TrkB and TrkC but not BDNF mRNA in neurochemically identified interneurons in rat visual cortex *in vivo* and in organotypic cultures. *Eur J Neurosci* 11:1179–1190.
65. Sakata K, et al. (2013) Role of activity-dependent BDNF expression in hippocampal-prefrontal cortical regulation of behavioral perseverance. *Proc Natl Acad Sci USA* 110: 15103–15108.
66. Itami C, Kimura F, Nakamura S (2007) Brain-derived neurotrophic factor regulates the maturation of layer 4 fast-spiking cells after the second postnatal week in the developing barrel cortex. *J Neurosci* 27:2241–2252.
67. Kvitsiani D, et al. (2013) Distinct behavioural and network correlates of two interneuron types in prefrontal cortex. *Nature* 498:363–366.
68. Xenos D, et al. (2017) Loss of TrkB signaling in parvalbumin-expressing basket cells results in network activity disruption and abnormal behavior. *Cereb Cortex* 28: 3399–3413.
69. Nelson ED, Monteggia LM (2011) Epigenetics in the mature mammalian brain: Effects on behavior and synaptic transmission. *Neurobiol Learn Mem* 96:53–60.
70. Besusso D, et al. (2013) BDNF-TrkB signaling in striatopallidal neurons controls inhibition of locomotor behavior. *Nat Commun* 4:2031.
71. Lein ES, et al. (2007) Genome-wide atlas of gene expression in the adult mouse brain. *Nature* 445:168–176.
72. Rossi MA, et al. (2012) Prefrontal cortical mechanisms underlying delayed alternation in mice. *J Neurophysiol* 108:1211–1222.
73. Grubbs FE (1969) Procedures for detecting outlying observations in samples. *Technometrics* 11:1–21.